Journal of Radiation Research, 2013, 54, 553–560
doi: 10.1093/jrr/rrs118 Advance Access Publication 4 January 2013

Quantitative analysis of in-air output ratio

Hisayuki MIYASHITA[1,2,*], Shogo HATANAKA[3], Yukio FUJITA[4], Shimpei HASHIMOTO[2,5], Atsushi MYOJYOYAMA[2] and Hidetoshi SAITOH[2]

[1]Tokyo Metropolitan Geriatric Hospital and Institute of Gerontorogy, Sakaecho 35-2, Itabashi-ku, Tokyo 173-0015, Japan
[2]Graduate School of Human Health Sciences, Tokyo Metropolitan University, Higashiogu 7-2-10, Arakawa-ku, Tokyo 116-8551, Japan
[3]St Luke's International Hospital, Akashicho 9-1, Chuo-ku, Tokyo 106-8560, Japan
[4]Tohoku University, Seiryocho 2-1, Aoba-ku, Sendai-city, Miyagi 980-8575, Japan
[5]Tokyo Metropolitan Cancer and Infectious Diseases Center, Komagome Hospital, Honkomagome 3-18-22, Bunkyo-ku, Tokyo 113-8677, Japan
*Corresponding author. Tel: +81(03)3964-1141; E-mail: miyashita-hisayuki@hs.tmu.ac.jp

(Received 9 April 2012; revised 6 November 2012; accepted 15 November 2012)

Output factor (S_{cp}) is one of the important factors required to calculate monitor unit (MU), and is divided into two components: phantom scatter factor (S_p) and in-air output ratio (S_c). Generally, S_c for arbitrary fields are calculated using several methods based on S_c determined by the absorbed dose measurement for several square fields. However, there are calculation errors when the treatment field has a large aspect ratio and the opening of upper and lower collimator are exchanged. To determine S_c accurately, scattered photons from the treatment head and backscattered particles into the monitor chamber must be analyzed individually. In this report, a simulation model that agreed well with measured S_c was constructed and dose variation by scattered photons from the treatment head and by backscattered particles into the monitor chamber was analyzed quantitatively. The results showed that the contribution of scattered photons from the primary collimator was larger than that of the flattening filter, and backscattered particles were affected by not only the upper jaw but also the lower jaw. In future work, a new S_c determination algorism based on the result of this report will be proposed.

Keywords: in-air output ratio; scattered photon; collision water kerma; backscattered particles; Monte Carlo method

INTRODUCTION

Determination of the monitor unit (MU) is required to deliver a prescribed absorbed dose to planning target volume (PTV). The output factor is one of the important parameters required to determine MU. According to Kahn *et al.*, the output factor is derived from two components [1, 2]: one is the phantom scatter factor (S_p)—the ratio of the dose rate of a given field to the dose rate of a reference field at the same depth. The other is the collimator scatter factor (S_c)—the ratio of output in air of a given field to that of a reference field. The collimator scatter factor is also called the 'head scatter factor' or the 'in-air output ratio', but the term 'in-air output ratio' and 'S_c' are used to describe the factor in this report.

According to the report of AAPM TG-74, S_c is defined as the ratio of collision water kerma in the free space of an arbitrary field to that of a reference field [3]. When charged particle equilibrium is established, collision water kerma may be an approximation of the absorbed dose. Generally, S_c is determined by absorbed dose measurement using miniphantom and ionization chambers for several square fields.

In clinical studies, S_c for arbitrary fields are calculated using the A/P [4] or other methods [5–7]. However there are calculation errors for both open and wedge fields with large aspect ratios [8, 9]. Furthermore S_c differs when the opening of the upper and lower collimator jaws is exchanged. This phenomenon is called collimator exchange effect (CEE) [9], and could be corrected using the 'field

mapping method' [9]. However, the field mapping method might overestimate S_c when the upper jaw is fixed and underestimate S_c when the lower jaw is fixed for the Varian machines.

To determine S_c accurately, scattered photons from the flattening filter, the primary collimator, jaws and backscatter to monitor chamber should be considered. Chaney *et al.* reported the fluence and energy spectrum of scattered photons from the treatment head [10]. However, they evaluated S_c using photon fluence instead of the absorbed dose or collision kerma so that the calculated S_c and the measured S_c did not agree well for the arbitrary field. On the other hand, some authors have experimentally evaluated the effect of backscattered particles to the monitor chamber. Duzenli *et al.* reported 'relative chamber reading' as the effect of backscattered particles using the telescope method [11]. Lam *et al.* calculated monitor backscatter factor based on the measurement of charge deposited in the target [12]. However, these reports gave nothing but backscatter phenomenon and are insufficient in terms of supplying quantitative evidence to agree with the actual S_c. Ding simulated S_c considering the variation of backscattered particles to the monitor chamber and compared this with measured data [13]. The report showed good agreement between simulated and measured S_c for not only square fields but also rectangular fields. However the Monte Carlo simulation was performed comprehensively and did not give individual information of scattered photons from head component and backscattered particles. In addition, it is time consuming and impractical for clinical use.

To calculate S_c for clinical fields with high accuracy and less computing time, a new S_c determination algorism considering the CEE phenomenon and the complex field shaped by a multi leaf collimator (MLC) is required. We assumed that S_c can be expressed with the next two functions. Dose variation by scattered photons from the treatment head can be regarded as a function of upper jaw, lower jaw and MLC opening. On the other hand, dose variation by backscattered particles into the monitor chamber can be regarded as a function of upper jaw opening. Therefore two functions must be analyzed individually. In this report, a simulation model that agreed well with measured S_c was constructed. And furthermore, dose variation by scattered photons from the treatment head and by backscattered particles into the monitor chamber was analyzed quantitatively.

MATERIALS AND METHODS

Measurement of S_c

Figure 1 shows the geometry of the S_c measurement. Ionization charges for several square fields were measured using a farmer type ionization chamber (TN-30013; Physikalisch-Technische Werkstätten, Germany) mounted in miniphantom. The miniphantom is cylindrical in shape, 4 cm in diameter and 20 cm in height, and set on the beam axis. The sensitive volume of the chamber was set at $SCD = 100$ cm and 10 cm in physical depth. Variation of the quality correction factor, k_Q, by field size can be ignored, therefore S_c for arbitrary field A is calculated using the following equation when the electrometer reading is $M(A)$:

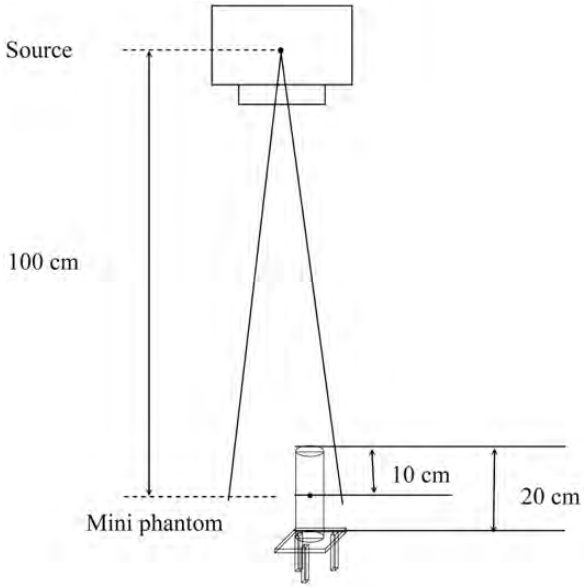

Fig. 1. Measurement geometry of in-air output ratio, S_c

$$S_c(A) = \frac{M(A)}{M(A_{ref})} \quad (1)$$

where A_{ref} is the reference field ($A = 10\ \text{cm} \times 10\ \text{cm}$).

Treatment head modeling and beam commissioning

Figure 2 shows the geometry of the treatment head of the Clinac 600C (Varian medical systems, USA), which generates 4 MV X-rays. Head components from the target to the isocenter were precisely coded using BEAMnrc [14]. The initial electron energy and spatial distributions on the target were adjusted by comparison between measured and calculated dose distributions. Their agreement was judged objectively using the method and criteria of Venselaar *et al.* [15].

Simulation of photons generated from the treatment head

Photons from the treatment head were sampled within a 0.5-cm radius circular region on the central axis at 100 cm from the target. Sampled photons were categorized by each

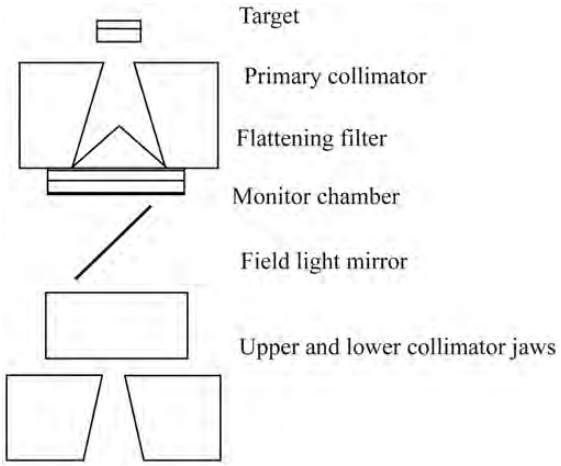

Fig. 2. Schematic diagram of treatment head of Clinac 600C (Varian)

accelerator head component where interaction took place using the 'latch' option.

Collision water kerma for the arbitrary field ${}_{\mathrm{col}}K(A)$ was calculated using information from sampled photons as follows:

$$ {}_{\mathrm{col}}K(A) = \int_{E_{\min}}^{E_{\max}} \Phi_E(A) \cdot E \cdot \frac{\mu_{\mathrm{en}}(E)}{\rho}\, \mathrm{d}E \qquad (2) $$

where Φ_E (A) is the photon fluence at energy E for field size A, and $\mu_{\mathrm{en}}(E)/\rho$ is the mass energy absorption coefficient of water, respectively.

To analyze the contribution of scattered photons to the collision water kerma, positions (x', y') of interaction between photons and the head component were calculated using the following equations:

$$ x' = x - \left\{ \left(\frac{SSD - z_{\mathrm{last}}}{w} \right) \times u \right\} \qquad (3) $$

$$ y' = y - \left\{ \left(\frac{SSD - z_{\mathrm{last}}}{w} \right) \times v \right\} \qquad (4) $$

where SSD is the distance from the target to the sampling plane (= 100 cm); z_{last} is the distance of the Z axis from the target to the position where the photon interaction took place; u, v, w is the direction cosine of scattered photons to the X, Y, Z axes; and (x, y) is the position on the sampling plane shown in Fig. 3.

Simulation of backscatter particles from jaws and mirror

Absorbed doses to air of monitor chamber for various jaw openings were calculated using the Monte Carlo simulation

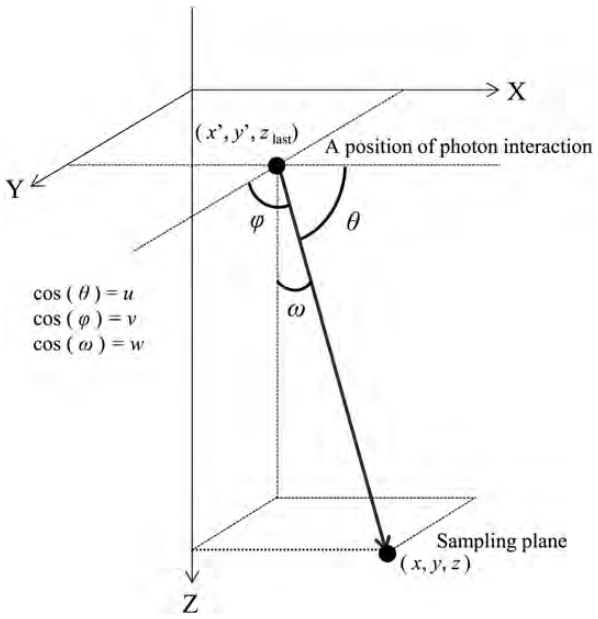

Fig. 3. Schematic diagrams to calculate positions of interaction between photon and head components

to analyze variation of the monitor chamber response by backscattered particles from jaws and mirror.

Calculation of S'_c, S_b and S_c

The ratio of collision water kerma S'_c (A) for the arbitrary field A to the reference field A_{ref} is calculated using the following equation:

$$ S'_{\mathrm{c}}(A) = \frac{{}_{\mathrm{col}}K_{\mathrm{p}}(A) + {}_{\mathrm{col}}K_{\mathrm{s}}(A)}{{}_{\mathrm{col}}K_{\mathrm{p}}(A_{\mathrm{ref}}) + {}_{\mathrm{col}}K_{\mathrm{s}}(A_{\mathrm{ref}})} \qquad (5) $$

where ${}_{\mathrm{col}}K_{\mathrm{p}}$ and ${}_{\mathrm{col}}K_{\mathrm{s}}$ are the collision water kerma of primary photons and that of scattered photons, respectively. ${}_{\mathrm{col}}K_{\mathrm{s}}$ was calculated as follows:

$$ {}_{\mathrm{col}}K_{\mathrm{s}} = {}_{\mathrm{col}}K_{\mathrm{s}}^{\mathrm{pcol}} + {}_{\mathrm{col}}K_{\mathrm{s}}^{\mathrm{ff}} + {}_{\mathrm{col}}K_{\mathrm{s}}^{\mathrm{jaws}} + {}_{\mathrm{col}}K_{\mathrm{s}}^{\mathrm{others}} \qquad (6) $$

where ${}_{\mathrm{col}}K_{\mathrm{s}}^{\mathrm{pcol}}$, ${}_{\mathrm{col}}K_{\mathrm{s}}^{\mathrm{ff}}$ ${}_{\mathrm{col}}K_{\mathrm{s}}^{\mathrm{jaws}}$ ${}_{\mathrm{col}}K_{\mathrm{s}}^{\mathrm{others}}$ are the collision water kerma of scattered photons from the primary collimator, flattening filter, jaws and other head components, respectively.

S_{b} is the variation of monitor chamber response by jaw opening, and is defined by the following equation:

$$ S_{\mathrm{b}}(A) = \frac{\dfrac{D_{\mathrm{front}}(A)}{D_{\mathrm{front}}(A) + D_{\mathrm{back}}(A)}}{\dfrac{D_{\mathrm{front}}(A_{\mathrm{ref}})}{D_{\mathrm{front}}(A_{\mathrm{ref}}) + D_{\mathrm{back}}(A_{\mathrm{ref}})}} \qquad (7) $$

where D_{front} is the absorbed dose to the air in the monitor chamber deposited by particles from the target, primary

collimator and flattening filter. D_{back} is the sum of the absorbed dose to air deposited by backscattered particles from the upper jaws D_{back}^{upjaws}, lower jaws $D_{back}^{lowjaws}$ and mirror D_{back}^{mirror} as per the following equation:

$$D_{back} = D_{back}^{upjaws} + D_{back}^{lowjaws} + D_{back}^{mirror} \quad (8)$$

On the other hand, D_{front} does not depend on jaw position, namely, field size A. Therefore $D_{front}(A)$ is constant and equal to $D_{front}(A_{ref})$. Thus, equation (7) can be converted into the following equation:

$$S_b(A) = \frac{D_{front}(A_{ref}) + D_{back}(A_{ref})}{D_{front}(A) + D_{back}(A)} \quad (9)$$

Considering the interaction between photons and treatment head components, S_c can be used to calculate the variation in collision water kerma in free space from scattered photons, and the monitor chamber response from backscattered particles. Therefore, the in-air output ratio by simulation S_c^{calc} can be calculated with the following equation:

$$S_c^{calc}(A) = S_c'(A) \cdot S_b(A) \quad (10)$$

For all simulations, 1.2×10^{11} incident electrons on the target were used to obtain statistical uncertainty of less than 2.0%.

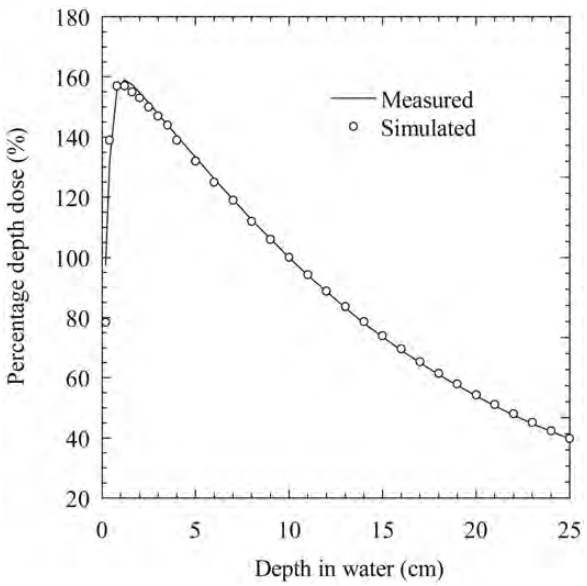

Fig. 4. Measured and simulated PDD in water for 10 cm × 10 cm field

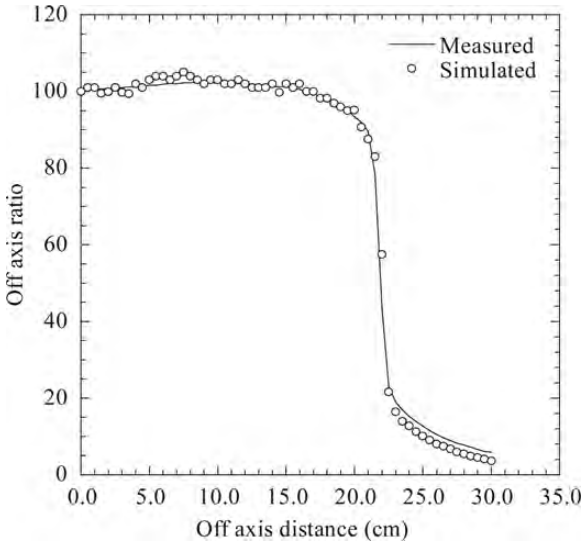

Fig. 5. Measured and simulated OAR at 10 cm depth in water for 40 cm × 40 cm field

Table 1. Criteria (confidence limit or DTA) of objective judgement for beam commissioning

	PDD		OAR		
Region	**1**	**2**	**2**	**3**	**4**
Venselaar *et al.*	2.0%	2.0 mm	2.0 mm	3.0%	30%
This report	1.1%	0.6 mm	1.3 mm	1.9%	25%

Region numbers were defined as: 1, points on the central beam axis beyond the depth of d_{max}; 2, points in the build-up region and penumbra; 3, points beyond d_{max}, within the beam but outside the central beam axis; 4, points off the geometrical beam edges and below shielding blocks.

RESULTS AND DISCUSSION

Commissioning results of beam model

Measured and simulated dose distributions are shown in Figs 4 and 5, and the confidence limit and distance to agreement (DTA) for each region is shown in Table 1. When incident electron energy was 4.0 MeV with 1.5% of full width half maximum (FWHM) energy spread and 0.3 cm of spatial FWHM, the confidence limit and DTA satisfied the criteria at all evaluation regions. Therefore, it is confirmed that the following simulation faithfully reproduced the actual beam.

Analyses of photons from head components

Collision water kerma of primary and scattered photons calculated by equation (2) for a square field are shown in

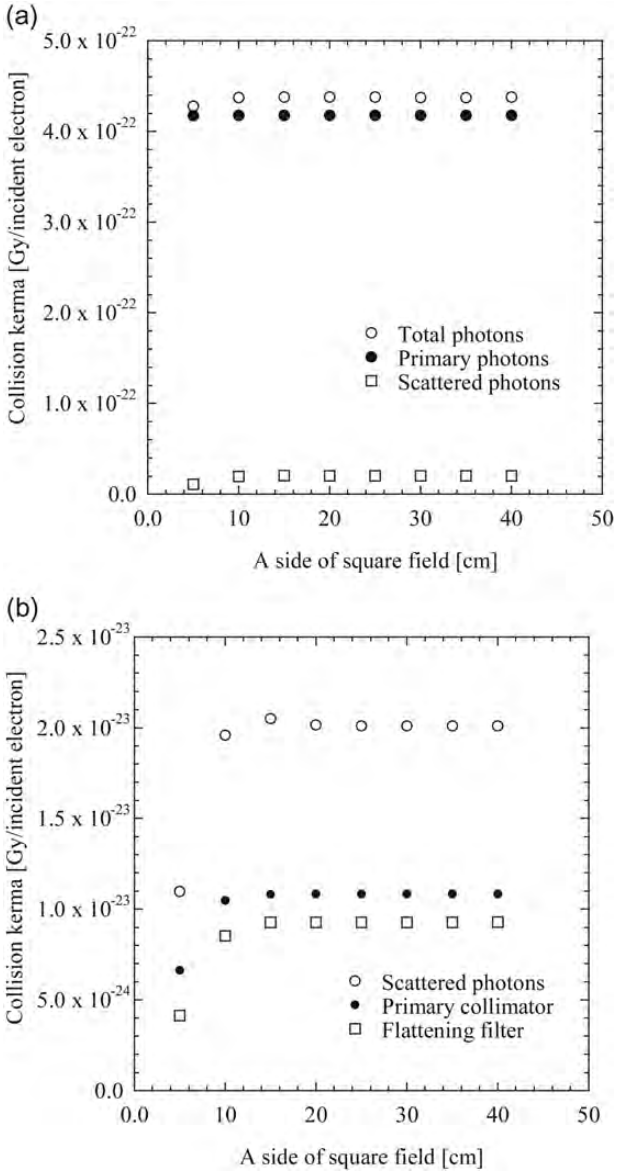

Fig. 6. Collision water kerma as a function of field size divided into (**a**) primary and scattered photons; (**b**) scattered photons from the primary collimator and flattening filter

Fig. 6(a). Collision water kerma of primary photons accounted for over 95.5% of the total, and did not depend on field size. On the other hand, collision water kerma of scattered photons increased slightly as the field size enlarged. Collision water kerma of scattered photons from each head component are shown in Fig. 6(b), and the percentage of collision water kerma from head components to total scattered photons are shown in Table 2. Collision water kerma from the primary collimator and flattening filter accounted for from 53.7–59.9 % and 38.2–46.3 % of total scattered photons, respectively. However, collision water kerma from collimator jaws and others were small amounts so could be ignored. Thus, it was obvious that scattered photons from the primary collimator and flattening filter affect S_c.

Table 2. Percentage of collision water kerma from head components to total scattered photons

	A side of square field (cm)			
Components	**5**	**10**	**20**	**40**
Primary collimator	59.9	53.2	53.6	53.7
Flattening filter	38.2	43.7	46.2	46.3
Others	0.19	0.31	0.20	0.00

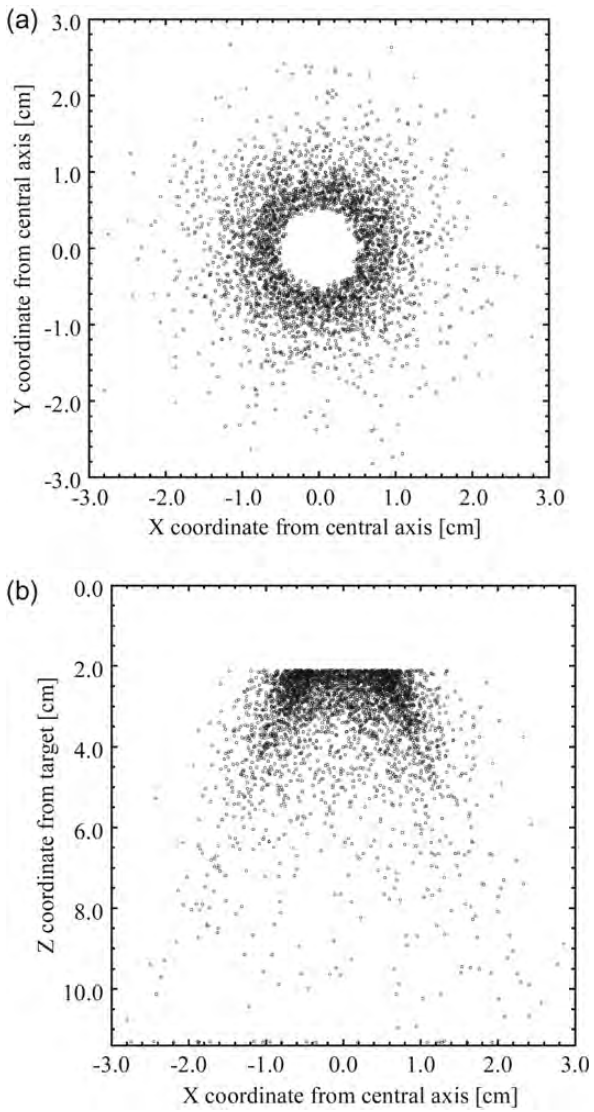

Fig. 7. Spatial distribution of interaction points of scattered photons at primary collimator (**a**) X–Y coordinate; (**b**) X–Z coordinate

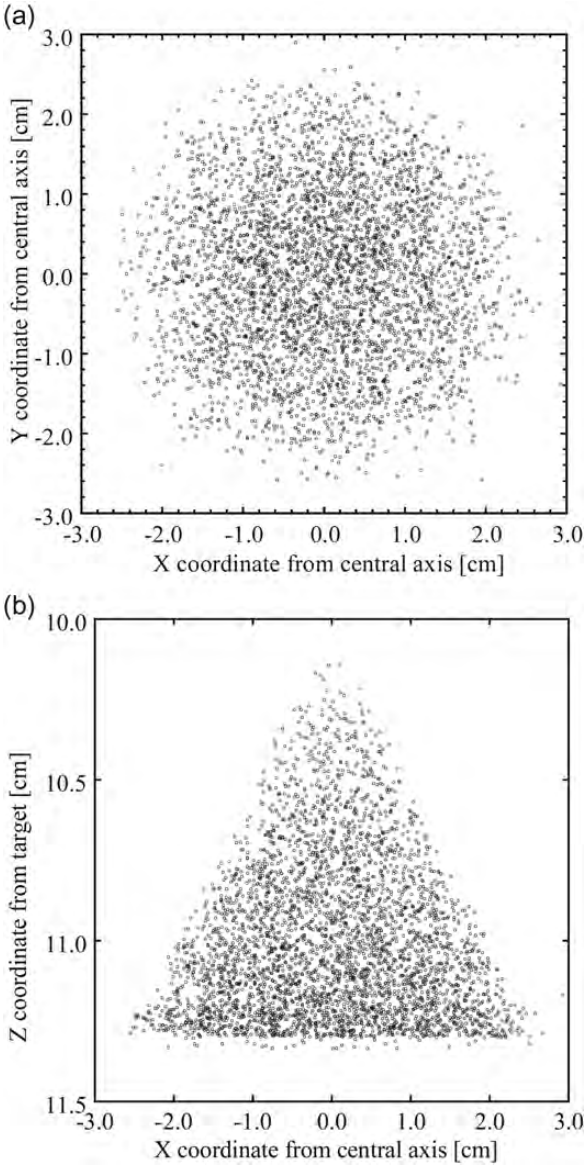

Fig. 8. Spatial distribution of interaction points of scattered photons at flattening filter (**a**) X–Y coordinate; (**b**) X–Z coordinate

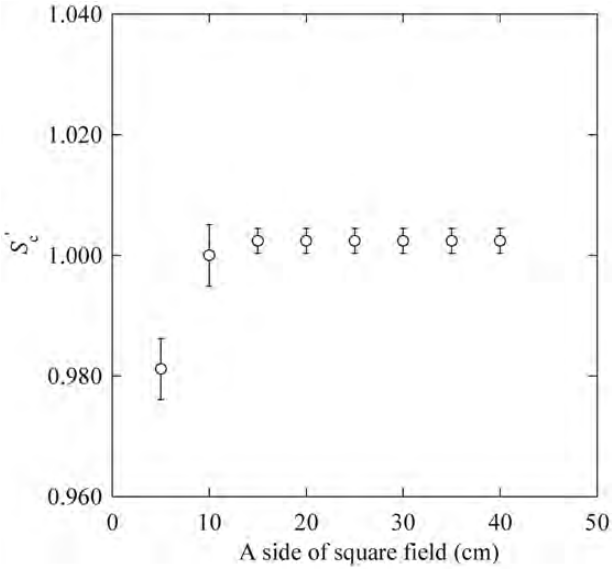

Fig. 9. S'_c as a function of field size

The spatial distribution of the interaction coordinate of scattered photons at the primary collimator and flattening filter as calculated by equations (3) and (4) is shown in Fig. 7 for the primary collimator and Fig. 8 for the flattening filter. The Interaction coordinate was distributed throughout and the shapes of the primary collimator and flattening filter were clearly discernible.

The S'_c calculated using equation (5) is shown in Fig. 9. S'_c increases from 0.981 for 5 cm × 5 cm to 1.002 for 15 cm × 15 cm. For this field range, S'_c depends on fluence of scattered photons from the primary collimator and flattening filter. On the other hand, in the field larger than 15 cm × 15 cm, the primary collimator and flattening filter can be seen fully from the point of calculation because they are not concealed by jaws.

Analyses of backscattered particles into the monitor chamber

The absorbed dose to air deposited by particles from the target side and back side in the monitor chamber is shown in Fig. 10(a). The contribution of particles from the target side was constant, however, the contribution of backscattered particles decreased as the jaws moved away from the central beam axis. The absorbed dose from backscattered particles accounted for 5.0% for 5 cm × 5 cm, and 1.0% for 40 cm × 40 cm fields of the total absorbed dose to air in the monitor chamber.

The absorbed dose to air by backscattered particles from the upper and lower jaws are shown in Fig. 10(b), and the percentage of total for several fields are shown in Table 3. Percentage of absorbed dose by the upper jaws compared with that of total backscattered particles decreased linearly as field size enlarged from 97.3% for 5 cm × 5 cm to 72.4% for 40 cm × 40 cm. On the other hand, the percentage of absorbed dose from lower jaws to that of total backscattered particles increased from 2.6% for 5 cm × 5 cm to 27.6% for 40 cm × 40 cm. Th absorbed dose from the mirror was a small amount and could be ignored.

S_b calculated using equation (9) is shown in Fig. 11. S_b increased from 0.956 to 1.033 as field size enlarged.

Evaluation of S_c^{calc}

Comparisons of measured and calculated S_c using equation (10) are shown in Fig. 12. The calculated and actual S_c agreed within 0.5% for several square fields. There are

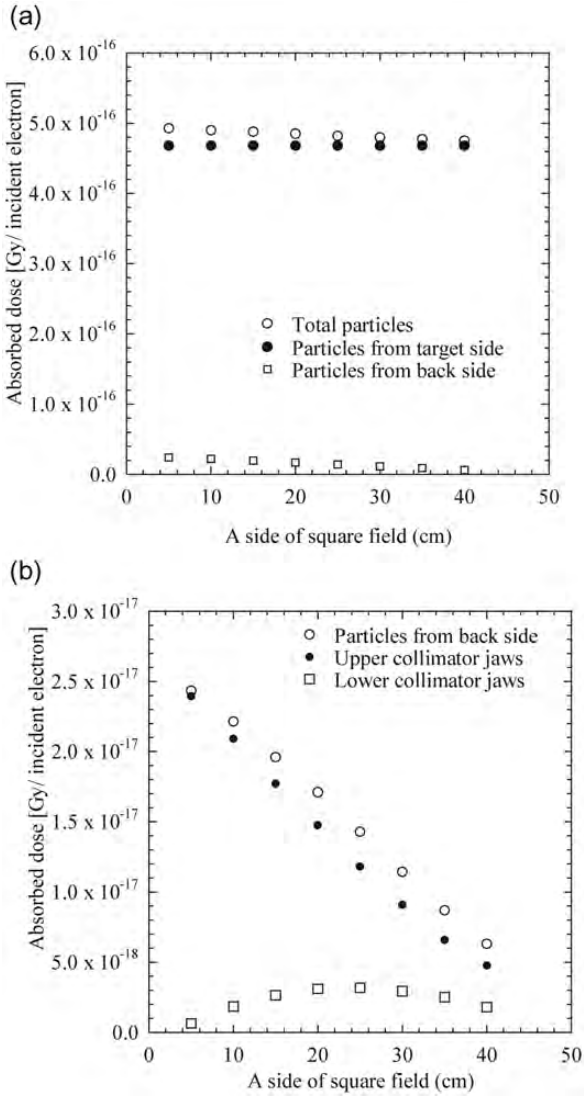

Fig. 10. Absorbed dose to air in monitor chamber as a function of field size divided into (**a**) particles from target and back side; (**b**) backscattered particles from upper and lower jaws

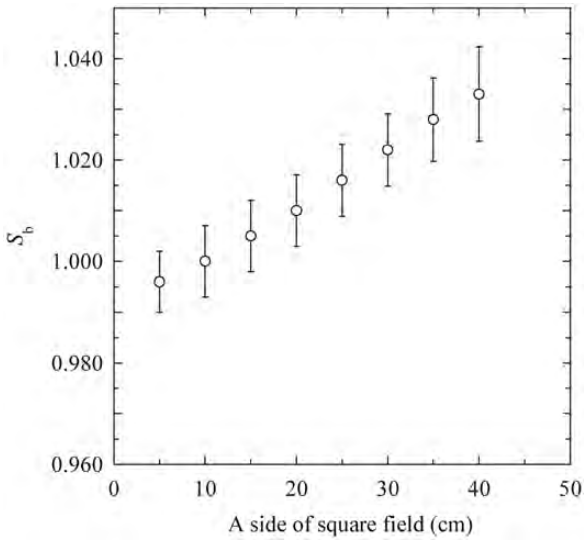

Fig. 11. S_b as a function of field size

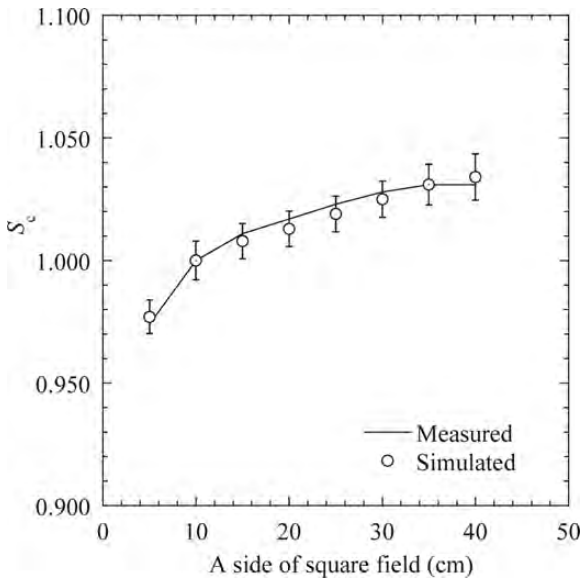

Fig. 12. Measured and simulated S_c as a function of field size

Table 3. Percentage of absorbed dose of backscattered particles from head components to total dose

	A side of square field (cm)			
Components	**5**	**10**	**20**	**40**
Upper collimator jaws	97.3	91.9	82.6	72.4
Lower collimator jaws	2.6	8.1	17.4	27.6

some reports about calculation of S_c based on scattered photons from the flattening filter [9, 16]. However, it is obvious that an accurate S_c cannot be calculated without scattered photons from the primary collimator and

Table 4. Comparison of each scatter factor for various square fields

	A side of square field (cm)			
Scatter factor	**5**	**10**	**20**	**40**
S'_c	0.981	1.000	1.002	1.002
S_b	0.996	1.000	1.010	1.033
Simulated S_c	0.977	1.000	1.013	1.034
Measured S_c	0.974	1.000	1.017	1.031

backscattered particles from jaws into the monitor chamber. Furthermore, the amount of scattered photons from the primary collimator is larger than that from the flattening filter. On the other hand, S_c is affected by variation of S_b for fields larger than 15 cm × 15 cm as is shown in Table 4.

CONCLUSION

To express S_c with two different functions, a Monte Carlo simulation model that agreed well with measured S_c was constructed. And dose variation by scattered photons from the treatment head and by backscattered particles into the monitor chamber was analyzed quantitatively.

The results showed that the contribution of scattered photons from the primary collimator was larger than that of the flattening filter, and backscattered particles were affected not only by the upper jaw but also the lower jaw. In future work, a new S_c determination algorism based on the result of this report will be proposed.

ACKNOWLEDGEMENTS

The authors wish to thank Kazuo Noda and Masahiro Uekusa, the chief radiological technologists of Fraternity Memorial Hospital for allowing use of the liner accelerator. The authors also wish to thank Varian Medical Systems for providing detailed drawings.

REFERENCES

1. Khan F, Sewchand W, Lee J *et al*. Revision of tissue-maximum ratio and scatter-maximum ratio concepts for cobalt 60 and higher energy x-ray beams. *Med Phys* 1980;**7**:230–7.
2. Khan F. *The physics of radiation therapy* (3rd ed.). Philadelphia: Lippincott Williams & Wilkins, 2003.
3. Zhu T, Ahnesjo A, Lam K *et al*. Report of AAPM Therapy Physics Committee Task Group 74: in-air output ratio, S_c, for megavoltage photon beams. *Med Phys* 2009;**36**:5261–91.
4. Sterling T, Petty H, Katz L. Automation of radiation treatment planning. *Brit J Radiology* 1964;**37**:544–50.
5. Day J. The equivalent field method for axial dose determinations in rectangular fields. *British Institute of Radiology* 1972;**11**:95–100.
6. Clarkson J. A note on depth dose in fields of irregular shape. *Brit J Radiology* 1941;**14**:265–8.
7. Bjarngard B, Siddon R. A note on equivalent circles, squares, and rectangles. *Med Phys* 1982;**9**:258–60.
8. Tatcher M, Bjarngard B. Head-scatter factors in rectangular photon fields. *Med Phys* 1993;**20**:205–6.
9. Kim S, Zhu T, Palta J. An equivalent square field formula for determining head scatter factors of rectangular fields. *Med Phys* 1997;**24**:1770–4.
10. Chaney E, Cullip T, Gabriel T. A Monte Carlo study of accelerator head scatters. *Med Phys* 1994;**21**:1383–90.
11. Duzenli C, McClean B, Field C. Backscatter into the beam monitor chamber: implications for dosimetry of asymmetric collimators. *Med Phys* 1993;**20**:363–7.
12. Lam K, Muthuswamy M, Ten-Haken R. Measurement of backscatter to the monitor chamber of medical accelerators using target charge. *Med Phys* 1998;**25**:334–8.
13. Ding G. An investigation of accelerator head scatters and output factor in air. *Med Phys* 2004;**31**:2527–33.
14. Rogers D, Faddegon B, Ding G *et al*. BEAM: a Monte Carlo code to simulate radiotherapy treatment units. *Med Phys* 1995;**22**:503–24.
15. Venselaar J, Welleweerd H, Mijnheer B. Tolerances for the accuracy of photon beam dose calculations of treatment planning systems. *Radiother Oncol* 2001;**60**:191–201.
16. Lam K, Muthuswamy M, Ten-Haken R. Flattening-filter-based empirical methods to parameterize the head scatter factor. *Med Phys* 1996;**23**:343–52.